



MIDDLE HOLOCENE CLIMATE VARIABILITY FROM A STALAGMITE FROM ALILICA CAVE (SOUTHERN BALKANS)

Eleonora Regattieri ^{1,2}, Ilaria Isola ³, Giovanni Zanchetta ^{1,3}, Andrea Tognarelli ¹,
John C. Hellstrom ⁴, Russell N. Drysdale ^{5,6}, Chiara Boschi ², Ivica Milevski ⁷, Marjan Temovski ⁸

¹Dipartimento di Scienze della Terra, University of Pisa, Pisa, Italy.

²Istituto di Geoscienze e Georisorse IGG-CNR, Pisa, Italy.

³Istituto Nazionale di Geofisica e Vulcanologia INGV, Pisa, Italy.

⁴School of Earth Sciences, University of Melbourne, Victoria, Australia.

⁵School of Geography, University of Melbourne, Victoria, Australia.

⁶EDYTEM, UMR CNRS 5204, Université de Savoie-Mont Blanc, Le Bourget du Lac Cedex, France.

⁷Institute of Geography, University of Skopje, Skopje, Republic of Macedonia.

⁸ICER, Institute for Nuclear Research, Hungarian Academy of Sciences, Debrecen, Hungary.

Corresponding author: E. Regattieri <eleonora.regattieri@unipi.it>

ABSTRACT: We present a stable isotope ($\delta^{13}\text{C}$ and $\delta^{18}\text{O}$) and growth rate record from a southern Balkans stalagmite, LID1, deposited between ca. 8.4 and 4.1 ka. Both stable isotope time series show significant changes at the centennial-millennial time scale, which are broadly consistent with variations in growth rate. The $\delta^{13}\text{C}$ signal and the growth rate appear related to soil-vegetation development over the cave catchment, influenced by regional temperature and hydrological variations. Also for the $\delta^{18}\text{O}$ record, a hydrological significance is proposed and particularly a dependence from the amount of precipitation at the cave site appears likely. Comparison of the multiproxy record from LID1 with regional hydroclimatic and temperature records shows both similarities and differences. Similarities appear related to the influences of large-scale atmospheric patterns such as the strength of the Siberian High and of the North Atlantic Oscillation, both exerting effects on local climate parameters like temperature, precipitation amount and seasonality. Differences arise from the complex interplay of different climatic regimes and of local conditions. Frequency analyses of the stable isotope time series shows periodicities similar to those related to solar activity, suggesting a solar modulation for the observed variability. Overall, the presented LID1 record adds a piece in the puzzle of the regional paleoclimatic framework for the Middle Holocene in the Mediterranean region.

Keywords: speleothem, Holocene, stable isotope, Balkans.

1. INTRODUCTION

The climate of the present interglacial, the Holocene (11.6 ka to the present, Walker et al., 2012), has been characterised by relatively stable conditions compared to the previous glacial period, but also by millennial- to centennial-scale fluctuations that affected the high and low latitudes of both hemispheres (e.g. Bond et al., 1997; Mayewski et al., 2004). A plethora of studies, including several compilations of Holocene paleoclimatic records, have aimed to reconstruct the spatial and temporal patterns of this short-term variability (e.g. Mayewski et al., 2004; Wanner et al., 2008, 2011). From this research, it is apparent that the variability in Holocene climate is expressed in a particularly complex regional pattern. Many studies particularly focus on the Mediterranean region and its surroundings (e.g. Roberts et al., 2008; Fletcher et al., 2013). In the Mediterranean, regional and global climatic change is commonly associated with variations in the amount and seasonality of precipitation (e.g. Giorgi & Lionello, 2008). These hydrological changes influence water availability, likely a crucial issue for the ancient civilizations that developed in the region. Indeed, the assessment of interactions be-

tween Holocene climate and humans is a classical issue of circum-Mediterranean paleoclimatic-archaeological investigations (e.g. Cremaschi et al., 2016; Magny et al., 2002; Bar-Matthew & Ayalon, 2011).

In the Mediterranean, lake-levels, lake-isotopes, speleothem and deep-sea sedimentary records (e.g. Magny et al., 2002; Roberts et al., 2008; Piva et al., 2008) suggest a distinction between an early Holocene characterized by conditions wetter than present and a later period with a drier climate (e.g. Jalut et al., 2009; Sadori et al., 2011; Giraudi et al., 2011). The transition between these two states seems to be characterized by sharp and short-amplitude climate changes with regards to both temperature and precipitation (e.g. Bar-Matthews & Ayalon, 2011; Giraudi et al., 2011). It occurred in a time span, the Middle Holocene (ca. 8.2 ka to 4.2 ka, following Walker et al., 2012), corresponding to continuing high summer insolation in the Northern Hemisphere, and with the boreal ice sheets no longer large enough to influence climate at hemispheric scale (Wanner et al., 2008). Comparison of paleoclimate records with climate-forcing time series suggests that changes in insolation related both to Earth's orbital variations and to solar variability likely played a role (e.g. Mayewski et al.,

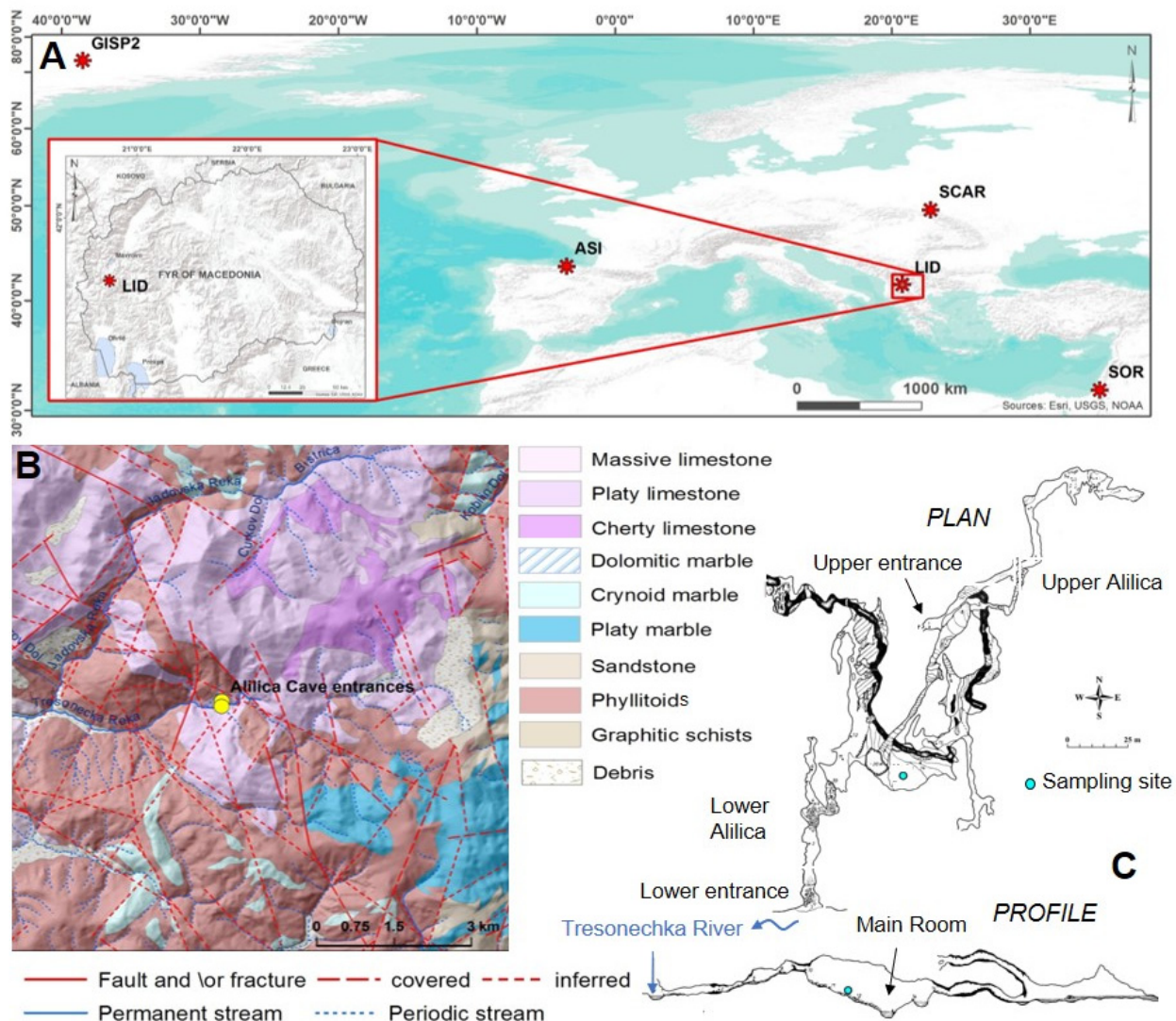


Fig. 1 - Geographic and geological setting of Alilica Cave: A - location of Alilica cave and of other sites mentioned in the text (LID= Alilica Cave, this study; ASI = Asiul Cave, Smith et al., 2016; SOR = Soreq Cave, Bar-Matthews et al., 2011; SCAR = Scarisacoara Cave, Perşoiu et al., 2017); B - geological setting of Alilica Cave (adapted from Petkovski & Ivanovski, 1980); C - map of Alilica Cave (adapted from Andonovski, 1980) and location of the sampling site.

2004, Debret et al., 2009, Wanner et al., 2011). Further, changes in North Atlantic Ocean circulation and variations in strength and direction of northern westerlies, with patterns similar to the atmospheric modes of the modern day North Atlantic Oscillation (NAO), have been proposed as drivers of Holocene variability in the Mediterranean (e.g. Perşoiu et al., 2017; Fletcher et al., 2013 Domínguez-Villar et al., 2008, Smith et al., 2016). An influence of low-latitude climate pattern has also been detected (Zanchetta et al., 2007).

In this work we present a stable isotope ($\delta^{13}\text{C}$ and $\delta^{18}\text{O}$) and growth rate record from a southern Balkans stalagmite, LID1, deposited between ca. 8.4 and 4.1 ka. Both stable isotope time series show significant changes at the centennial time scale, which are broadly consistent with variations in growth rate. We investigate the

climatic and environmental meaning of the proxies, the timing and periodicity of the variability and, through comparison with other records, its regional or local significance. The aim is to reconstruct the climate of the area during the Mid-Holocene and the potential links with regional and global climatic patterns.

2. STUDY SITE

2.1. Cave setting

Alilica Cave is located on the North side of the Tresonechka River Valley, in the Bistra Mountain range, within the Mavrovo National Park, in the Former Yugoslavian Republic of Macedonia (F.Y.R.O.M., Macedonia hereinafter, Fig. 1). The cave is developed in Mesozoic limestone of the Western Macedonian Geotectonic Unit

(Petkovski & Ivanovski, 1980; Karamata, 2006). It is 590 m long, with a maximum elevation range of 130 m (Andonovski, 1980). The cave is interested by significant speleothem deposition and comprises two different levels (Lower and Upper Alilica), connected by vertical passages ca. 90 m deep. The Lower Alilica opens at river level, at 1450 m a.s.l. The entrance is characterised by the accumulation of fluvial sand and gravel, which after periods of intense flooding block the entrance to the cave. The catchment of Alilica Cave is not well defined. However, it is likely that the cave drains the southwestern slope of the Bistra mountain, which is covered by a beech (*Fagus sylvatica*) forest up to 1600 m a.s.l. Above 1600 m a.s.l., there is a bare karstic plateau, with sparse grassland and the presence of glacial deposits (Petkovski & Ivanovski, 1980; Andonovski et al., 1998). All plants belong to the C3-type vegetation category.

Stalagmite LID1 (Fig. 2) was collected already broken in the lower part of Alilica Cave. The cave showed active dripping at time of collection and active speleothem growth was apparent.

2.2. Local climate

The climate in the area is sub-Mediterranean (Panagiotopoulos et al. 2013), with the greater part of the annual precipitation falling in the colder part of the year (autumn and winter). In the 1300-1650 m a.s.l. altitudinal range, where Alilica Cave and its catchment are located, the mean precipitation amount is ca. 1050 mm/yr. This altitude belt is the wettest climatic zone in Macedonia. The mean annual precipitation in the Mavrovo National Park is ca. 1250 mm (information from Mavrovo National Park web-site; [www. http://nmpmavrovo.org.mk](http://nmpmavrovo.org.mk)).

Moisture availability is linked mostly to cyclogenesis within the Mediterranean, especially occurring in the Gulf of Genoa. Cyclones originating there move southward following the Mediterranean storm trajectories (Reale & Lionello, 2013; Dünkelloh & Jacobeit, 2003; Ulbrich et al., 2012). As winter cyclogenesis in the Gulf of Genoa is associated with north-westerly storm tracks, an influence of North Atlantic atmospheric patterns is observed in the southern Balkan region, and there is a well-known negative correlation between the North Atlantic Oscillation (NAO) strength and winter precipitation (Ulbrich et al., 2012; López-Moreno et al., 2011). Other large-scale atmospheric patterns also have an influence on Mediterranean cyclogenesis. For example, positive anomalies of the Siberian High (a semi-permanent and quasi-stationary anticyclonic centre located in northern Eurasia, dominant in the boreal winter season) have a relationship with enhanced cyclogenesis and precipitation in the Mediterranean. Conversely, precipitation has been found to be inversely related to the strength of the Siberian High over almost all of Eastern Europe during the boreal winter, as well as over a large part of continental Asia (Rogers, 1997; Panagiotopoulos et al., 2005). The activity of the Siberian High is also positively related to an increase of the snow cover over all of Eurasia, especially in the early winter season (Cohen & Entekhabi, 1999). In spring and summer, the influence of large-scale climatic patterns is low and cyclogenesis

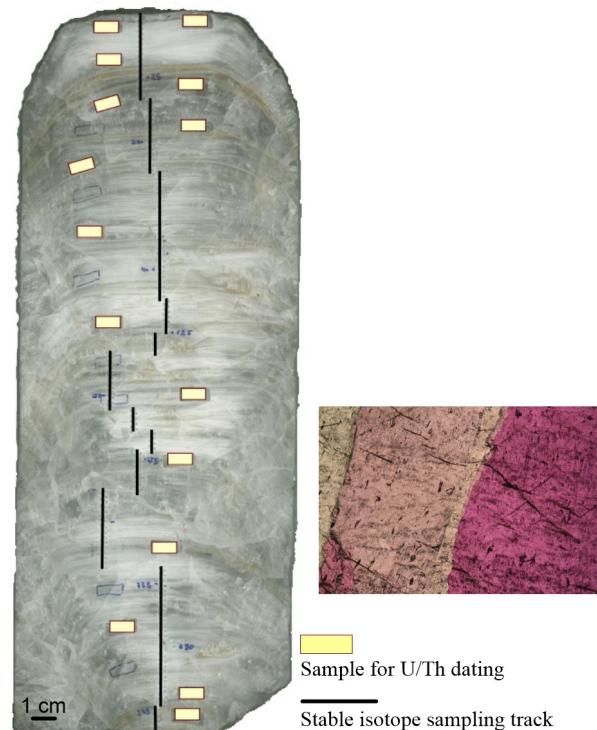


Fig. 2 - Stalagmite LID1 with reported the subsampling for stable isotope analyses and for ages determination. On the right a microphotograph of thin section (2.5X, crossed nicols) is reported.

over land, where local thermal trough systems play a major role, becomes more frequent and it is related to the local topography (Trigo et al., 2002). Summer dry conditions are related to the expansion of the Azores High, which in turn is influenced by the strength of the boreal monsoon system (Xoplaki et al., 2003). The annual cycle of temperature regime shows two distinct separate seasons: warm and dry summer and relatively cold winter connected with transitional spring and autumn. Mean summer temperature is of $\sim 25^{\circ}\text{C}$. Mean winter temperature varies around $\sim 3^{\circ}\text{C}$. The mean annual temperature is ca. 16°C . The winter temperature is not significantly correlated with NAO index (Ulbrich et al., 2012). Cold outbursts of north easterly sourced air masses can occur during the winter season and are linked to advection of polar air stimulated by the strengthening of the Siberia High (Panagiotopoulos et al., 2005).

3. MATERIAL AND METHODS

3.1. Sample description and petrography

Stalagmite LID1 is ca. 28 cm long and 11 cm wide (Fig. 2). It is candle-shaped and made up of white to translucent calcite, with no evidence of growth interruptions. It presents continuous, flat laminations, particularly apparent in the growth axis portion of the sample (Fig. 2).

Analyses of thin sections show that the dominant

fabric of LID1 is compact columnar calcite, with no evidence of annual lamination (Fig. 2). Crystals are large (up to 1 mm in length), have a regular shape, flat edges, elongated terminations and few crystal defects (Fig. 2).

3.2. Subsampling and stable isotope analyses

The stalagmite was cut longitudinally and one of the halves was hand-polished and subsampled along the growth axis for stable isotope ($\delta^{13}\text{C}$ and $\delta^{18}\text{O}$) analyses. In some portions, the drilling line was shifted laterally by a few mm, to avoid cracks and holes present on the surface. Subsampling was performed at 1-mm increments using a milling machine with a 1 mm-diameter drilling bit at the INGV (Institute of Geophysics and Volcanology, Pisa, Italy) laboratory, producing 285 subsamples. For U/Th dating, 15 solid prisms of ca. 150 mg (ca. 2 mm wide along the lamina and 1 mm thick on growth axis) were taken with a hand dental drill. Stable isotope analyses were made with a Gas Bench II (Thermo Scientific) coupled to a Delta XP continuous-flow isotope-ratio mass spectrometer at the Institute of Geosciences and Earth Resources of the Italian National Research Council (IGG-CNR, Pisa). Samples were digested for one hour in 105% phosphoric acid at 70 °C. Measurements were made on the evolved CO_2 gas. Results were normalized to the Vienna Pee Dee Belemnite scale using a set of internal working standards, calibrated among different laboratories and against the international standards NBS18 and NBS19. Mean analytical precision is 0.15‰ and 0.10‰ (2σ) for $\delta^{18}\text{O}$ and $\delta^{13}\text{C}$, respectively.

3.3. U/Th dating and age modelling

The U/Th dating was performed at the School of Earth Sciences at the University of Melbourne, Australia, following the method of Hellstrom (2003). Briefly, samples were dissolved and a mixed ^{236}U - ^{233}U - ^{229}Th spike was added prior to removal of the carbonate matrix with ion-exchange resin. The purified U and Th fraction diluted in nitric acid was introduced to a multi-collector inductively coupled plasma mass spectrometer

(MC-ICPMS, Nu-Instruments Plasma). The $^{230}\text{Th}/^{238}\text{U}$ and $^{234}\text{U}/^{238}\text{U}$ activity ratios were calculated from the measured atomic ratios using an internally standardized parallel ion-counter procedure and calibrated against the HU-1 secular equilibrium standard. Correction for detrital Th content was applied following the method described by Hellstrom, 2006. This method stratigraphically constrains the $^{230}\text{Th}/^{232}\text{Th}$ activity ratio ($^{230}\text{Th}/^{232}\text{Th}$)_i at the time of sample deposition, i.e. a sequence of true ages down the growth axis of a stalagmite or flowstone must become progressively older regardless of their relative degree of detrital contamination. A default initial activity ratios of detrital thorium ($^{230}\text{Th}/^{232}\text{Th}$)_i of 1.5 ± 1.5 has been employed here. The median value of 1.5, with a log-normal distribution corresponding to a 95% confidence interval of plus or minus a factor of 10, appears indeed to adequately cover the distribution of all speleothem ($^{230}\text{Th}/^{232}\text{Th}$)_i in the compilation of 50 speleothem records presented by Hellstrom (2006).

All the speleothem ages are expressed as 'before the year 2000 CE'. An age-depth model was constructed with a Bayesian statistical procedure using the software Stal-Age (Scholz & Hoffmann, 2011).

3.4. CWT analyses

The continuous wavelet transform (CWT, Daubechies, 1990) is a multi-resolution method used for time-series analyses. In general, the CWT analysis can be applied to all time or spatial series representing a non-stationary process, with the aim to investigate changes in their periodic components. Particularly, studies using WT analysis have indicated its suitability to investigate periodic components of the climatic system and their changes along the time (e.g. Debret et al., 2009). CWT was performed on $\delta^{18}\text{O}$ and $\delta^{13}\text{C}$ data series for the whole period of LID1 growth, employing a self-implemented Matlab code described in Tognarelli et al. (2018) and Tognarelli (2018). No filtering was performed before the wavelet analysis in order to preserve the original frequency content of the input data. Only a linear interpolation is applied to the data to produce a regular

Sample ID	Depth (mm)	^{238}U ng/g	$^{230}\text{Th}/^{238}\text{U}$	$^{234}\text{U}/^{238}\text{U}$	Age uncr (ka)	$^{232}\text{Th}/^{238}\text{U}$	$^{230}\text{Th}/^{232}\text{Th}$	Age cr (ka)	2se (ka)
LID1-4	4	14	0.0771	1.6865	5.075	0.006889	11.2	4.421	0.777
LID1A	5	23	0.0796	1.6962	5.212	0.008068	9.9	4.455	0.914
LID1-17	17		0.0753	1.7055	4.895	0.005676	13.3	4.372	0.554
LID1-29	29	13	0.1124	1.6647	7.570	0.038568	2.9	3.748	3.962
LID1B	32	16	0.1231	1.6705	8.287	0.028024	4.4	5.555	2.811
LID1-44	44		0.1242	1.6633	8.397	0.049877	2.5	3.431	5.169
LID1-54	54	20	0.1104	1.7127	7.216	0.022488	4.9	5.069	2.177
LID1-85	85		0.1059	1.6617	7.132	0.004379	24.2	6.732	0.447
LID1-120	120	21	0.1079	1.6666	7.250	0.006593	16.4	6.635	0.700
LID1-150	150		0.1176	1.6859	7.830	0.004966	23.7	7.379	0.490
<i>LID1-177*</i>	177	13	<i>0.1358</i>	<i>1.6240</i>	<i>9.448</i>	<i>0.057362</i>	2.4	<i>3.502</i>	<i>6.158</i>
LID1-210	210		0.1501	1.6124	10.564	0.050741	3.0	5.368	5.413
LID1C	268	30	0.1300	1.6263	9.016	0.003459	37.6	8.701	0.732
LID1-278	278		0.1338	1.6487	9.156	0.022286	6.0	6.968	2.227

Tab. 1- Corrected (in bold) and uncorrected U/Th ages for LID1 stalagmite. The activity ratios have been standardized to the HU-1 secular equilibrium standard, and ages calculated using decay constants of 9.195×10^{-6} (^{230}Th) and 2.835×10^{-6} (^{234}U). Depths are mm from top. The age* in italics was rejected as an outlier.

sampling over time and a default Δt of 1 yr is used as sample rate, as this minimum value guarantees that no extraneous frequency components are introduced in the data (Tognarelli et al., 2018). The Morlet complex wavelet is used to compute the wavelet spectra showed in Fig. 5.

4. RESULTS

4.1. Chronology and growth rate

The 15 U/Th ages obtained for LID1 stalagmite range from 8.70 ± 0.73 ka to 4.42 ± 0.78 ka. All the samples display a low U content (average 10 ppb; Table 1) and a significant detrital Th contamination (average $^{230}\text{Th}/^{232}\text{Th} = 10.9$, Table 1). This leads to the rather high temporal uncer-

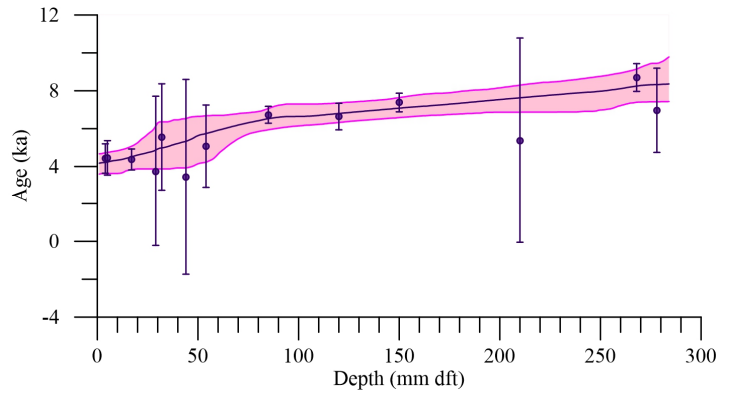


Fig. 3 - Age-Depth Model. The pink shading indicates the 95% confidence interval, dft means distance from top.

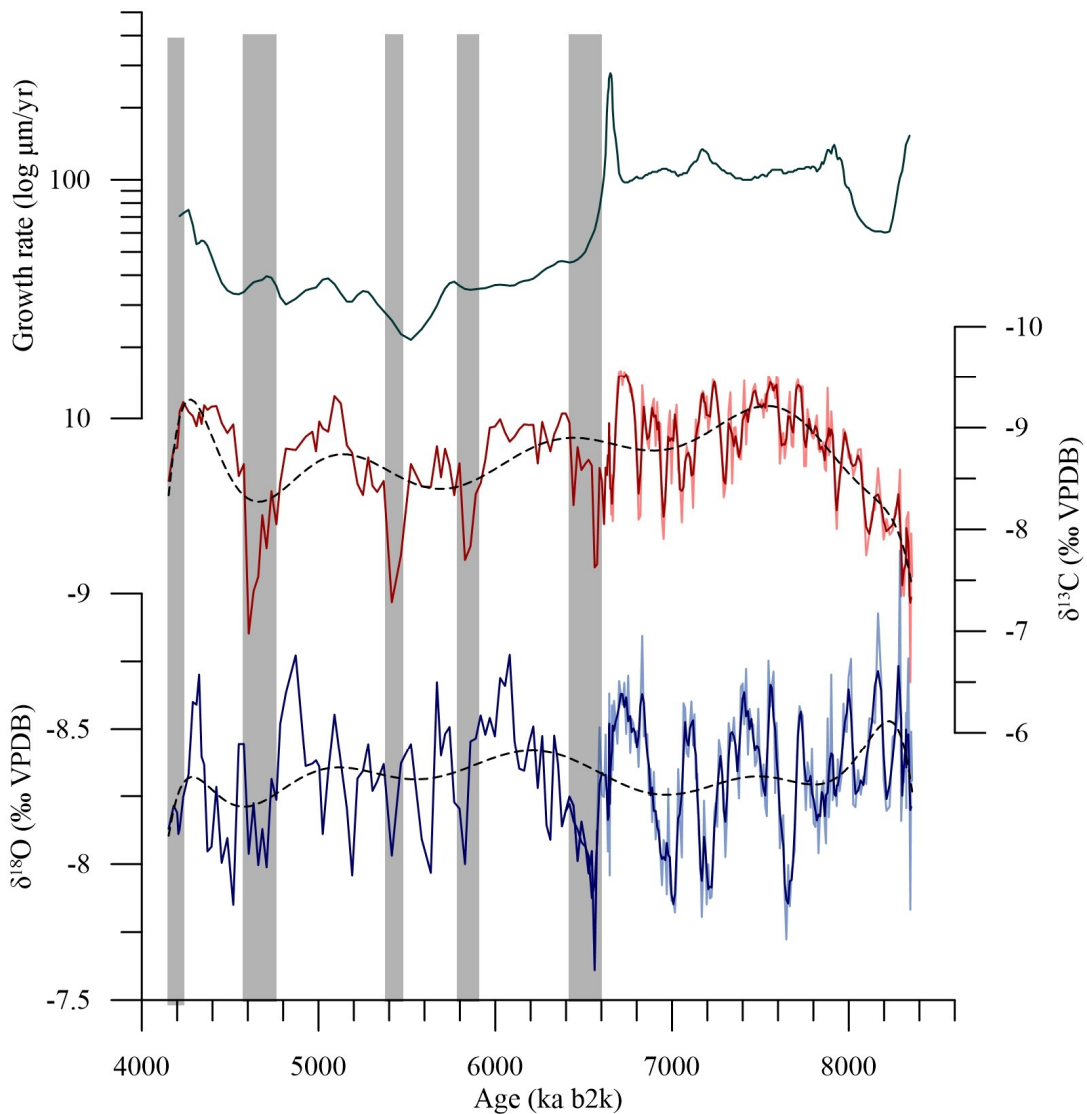


Fig. 4 - Stable isotope and growth rate results for stalagmite LID1. Grey bars indicate coherent intervals of increased isotope composition for both the $\delta^{13}\text{C}$ and the $\delta^{18}\text{O}$ record. In the older portion of the record, individual values are reported as lighter line, whereas the thick line is a 3pt moving average. Note that y axes for $\delta^{18}\text{O}$ and $\delta^{13}\text{C}$ are reversed.

tainty associated with the age determinations (Table 1). In LID1, ages were almost in stratigraphical order within the associated uncertainties, except for one age which was rejected as an outlier (Table 1). According to the age model (Fig. 3), the stalagmite grew between 8.36 ± 1.18 ka and 4.15 ± 0.56 ka. The average temporal resolution of the stable isotope record is ~ 15 yr, changing from a mean value of ~ 10 yr before ca. 6.6 ka to ~ 20 yr afterwards. The growth rate (Fig. 4) shows a major change around ca. 6.5 ± 0.54 ka. Prior to this, it shows an average value of ~ 100 $\mu\text{m}/\text{yr}$, with a small decrease to ~ 60 $\mu\text{m}/\text{yr}$ between ca. 8.2 ± 0.85 ka and 8.0 ± 0.9 ka and a spike toward increased growth rate at 6.6 ± 0.6 ka. After 6.5 ± 0.6 ka, the growth rate is lower, averaging ~ 35 $\mu\text{m}/\text{yr}$, with an interval of further reduction (~ 18 $\mu\text{m}/\text{yr}$) between ca. 5.7 ± 1.3 ka and 5.3 ± 1.3 ka. After ca. 4.5 ± 0.63 ka growth rate slightly increases again, to reach values of ~ 70 $\mu\text{m}/\text{yr}$ toward the end of the record (Fig. 4).

4.2. Stable isotopes

Stable isotope time series are shown in Fig. 4. The $\delta^{18}\text{O}$ ranges from -7.61 to -9.16 ‰ whereas $\delta^{13}\text{C}$ ranges between -6.50 and -9.56 ‰. Both stable isotope time series show significant variability at multi-decadal-to-centennial time scales. On the centennial time scale, a certain degree of similarity is apparent between the two isotope series, except for the beginning of the record,

where the $\delta^{13}\text{C}$ shows a trend of decreasing values, which is not present in the oxygen record (Fig. 4). The $\delta^{13}\text{C}$ values decrease from the onset of deposition until ca. 7.6 ± 0.7 ka, then values become more stable but with a slight trend toward more positive $\delta^{13}\text{C}$. Between 6.7 ± 0.6 ka and 6.4 ± 0.5 ka there is an interval of significantly increased values. Afterwards, the $\delta^{13}\text{C}$ series became again more stable but with significant and abrupt periods of more positive values between 6.0 ± 0.9 ka and 5.7 ± 1.2 ka, between 5.6 ± 1.3 ka and 5.2 ± 1.3 ka and between 4.8 ± 1.0 ka and 4.6 ± 0.7 ka (Fig. 4). The $\delta^{18}\text{O}$ series shows a stronger variability. Values greatly oscillate between 8.4 ± 1.2 ka and 6.6 ± 0.5 ka, with significant centennial intervals of more positive values apparent at 7.6 ± 0.7 ka, 7.2 ± 0.6 ka and 6.9 ± 0.5 ka. At ca. 6.6 ± 0.6 ka $\delta^{18}\text{O}$ values abruptly increase to their most positive, then steeply decrease again until ca. 6.2 ± 0.7 ka (Fig. 4). This interval of enriched $\delta^{18}\text{O}$ composition corresponds to a similar increase in the $\delta^{13}\text{C}$ record and to the strongest decrease in the growth rate (Fig. 4). Since ca. 6.7 ka, the variability of the $\delta^{18}\text{O}$ record appears more consistent with that of the carbon record, though oxygen values oscillate to a greater extent (Fig. 4).

4.3. Frequency analyses

The real wavelet spectra for the $\delta^{18}\text{O}$ and $\delta^{13}\text{C}$ series is shown in Figure 5. The black line indicates the

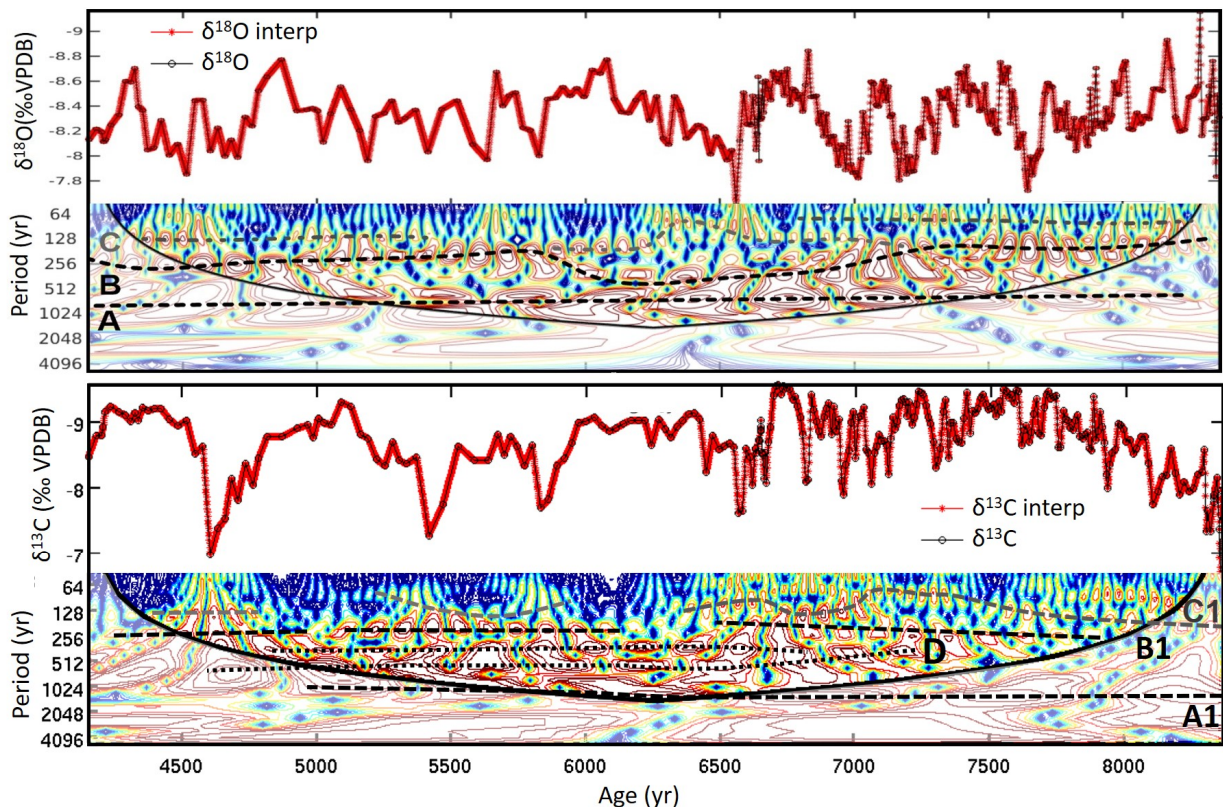


Fig. 5 - Interpolated oxygen (a-top panel) and carbon (b-bottom panel) time series of LID1 and respective real wavelet spectra. Letters indicate the main trends (see section 5.4 for details)

cone of influence (COI). It delimits the spectrum in two regions: the portion below the black line can be affected by edge effects and may show frequencies that are not significant due to the total length of the record (Tognarelli et al., 2018). In our case, periodicities longer than ~1000 yr are not significant (Fig. 5). Due to the rather large temporal uncertainty associated to the stable isotope record, periodicities shorter than 200 yr also should be considered with caution. From the wavelet spectrum, three main trends can be easily recognized in the analyses of the oxygen time series (Fig. 5a). A pervasive and rather constant periodicity centred on approximately 1000 yr is apparent throughout the record (Trend A in Fig. 5a). It appears stable and intense especially before ca. 5-6 ka, then shifted slowly to longer periodicities of ~1200-1500 yr, though this periodicity is not fully significant as it falls below the COI (Fig. 5a). At higher frequencies, a significant periodicity of ~200 yr is apparent (Trend B in Fig. 5a). This periodicity is stronger for the two extremities of the record, then decreases in the middle portion (i.e. between ca. 7.2 ka and 6 ka), where a lower frequency (~400 yr) is apparent. A third trend (C in Fig. 5a), less stable and intense, is centred between frequencies of ~75 - 100 yr. Also this trend shows a shift in the middle portion of the record, where it becomes weaker and slightly shifts to shorter periodicity (Fig. 5a). The real wavelet power spectrum for the carbon record shows less defined trends (Fig. 5b). Similar to the oxygen record, a periodicity of around 1000 yr is present from the beginning of the record to ca. 5000 yr (Trend A1 in Fig. 5b), though less defined and weaker especially in the middle portion of the record. At higher frequencies, a broad power band of 400-750 yr is apparent from ca. 7200 yr onward (Trend D, Fig. 5b). As for the oxygen, pervasive and with variable intensity periodicities of 200-250 yr and 75-120 yr can be recognized throughout the record (Trends B1 and C1 in Fig. 5b).

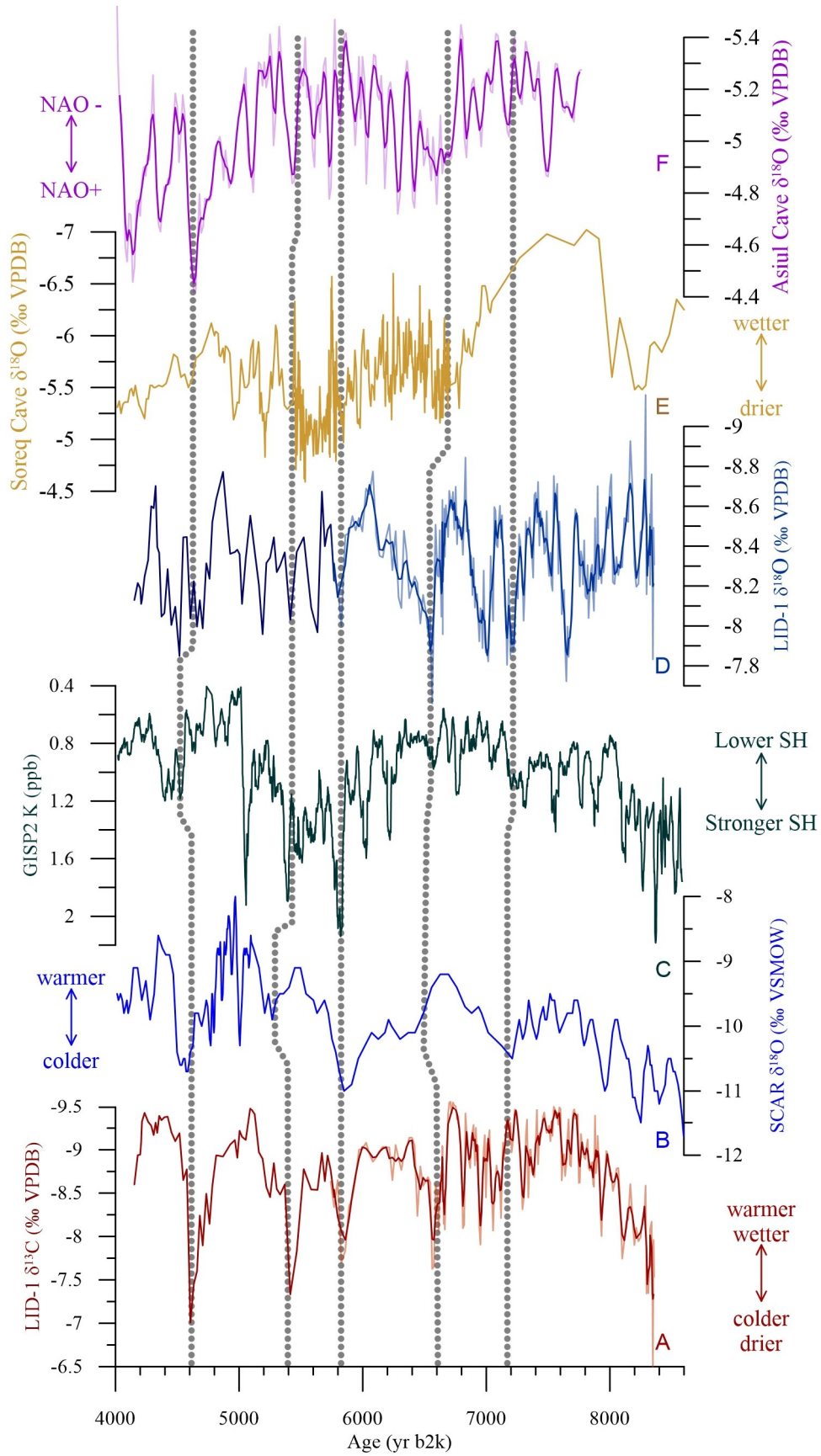
5. DISCUSSION

5.1. The $\delta^{13}\text{C}$ record

Speleothem $\delta^{13}\text{C}$ values arise from the complex interplay of changes in soil CO_2 production and content, closed versus open system dissolution of carbonates in the soil/bedrock system, hydrological routing of water along the pathway to the drip point and/or solution degassing (e.g. Fairchild et al., 2006; Bajo et al., 2017). The pollen records from Lakes Prespa and Ohrid, both located in Macedonia, show that altitudes comparable to that of Alilica Cave remained relatively wooded throughout the middle Holocene (Panagiotopoulos et al., 2013; Sadori et al., 2016), thus likely also the lower part of the Alilica catchment was characterized by a well-developed forest soil during the whole growth period of stalagmite LID1. In temperate settings with well-developed soil, increasing speleothem $\delta^{13}\text{C}$ values are often related to a decrease in CO_2 supply from soil biological activity, due to a reduction in rainfall and/or cooler climate (e.g. Genty et al., 2001a; Regattieri et al., 2014). Reduction in water recharge can also produce degassing along the karst network, resulting in higher $\delta^{13}\text{C}$ of drip water and speleothem (Fairchild et al., 2006). Conversely, more

negative carbon isotope values are related to an increase in soil development and productivity and to enhanced recharge, occurring under warmer and wetter conditions. Unpredictable fractionation of carbon isotopes can arise also from kinetic effects, when calcite precipitates out of isotopic equilibrium (Mickler et al., 2006). However, this is unlikely for LID1, which does not show petrographic features indicating major changes in the condition of precipitation (e.g. Frisia et al., 2000).

Figure 6 shows the comparison between LID1 $\delta^{13}\text{C}$ and the $\delta^{18}\text{O}$ record of ice preserved within the Scărișoara Cave (SCAR hereinafter), in NW Romania (Perșoiu et al., 2017). The SCAR ice provides a well-dated and high-resolution winter temperature record for Eastern Central Europe, because the $\delta^{18}\text{O}$ of cave ice reflects changes in air temperature during ice formation (September through December). Noteworthy, there is a general similarity with the LID1 $\delta^{13}\text{C}$ record, particularly for the initial trend and for colder intervals centred at ca. 7.1 ka, 6.5 ka, 5.8 ka, 5.4 ka and 4.5 ka which correspond to a trend toward more negative $\delta^{13}\text{C}$ and to more positive $\delta^{13}\text{C}$ spikes, respectively (Fig. 6). Cold conditions in Eastern and South Europe results from the interplay of northward intrusion of moisture carried by Mediterranean cyclones (Perșoiu et al., 2017) and by increased frequency of outbreaks of cold air from the northeast over the Aegean Sea, coincident with strengthening of the Siberian High (Rohling et al., 2002). Strengthening of the Siberian High is also related to winter drier conditions and early winter increased snow cover in central and eastern Europe (Panagiotopoulos et al., 2005; Cohen & Entekhabi, 1999). The K content from a Greenland ice core is considered to be positively correlated with pressure anomalies over Siberia (Meeker & Mayewski, 2002). Thus, periods with enhanced advection of polar air (i.e. stronger Siberian High) and increased southward penetration of north-easterly cold air masses should be marked by increased K concentration (e.g. Rohling et al., 2002). Comparison of the LID1 $\delta^{13}\text{C}$ records with potassium content from Greenland ice (core GISP2, Mayewski et al., 1997, Fig. 6) shows interesting similarities, both for the general trend and for some spikes in K content, which appear coincident, within combined uncertainty to cold/dry periods expressed by the LID1 carbon record and to colder intervals in the SCAR record (Fig. 6). This similarity is more remarkable during the second part of the record (after ca. 6.6 ka, e.g. at 5.8 ka and 4.5 ka). Overall, the observed similarities suggest that the $\delta^{13}\text{C}$ signal of LID1 stalagmite is mostly related to soil-vegetation development over the cave catchment, and that the latter is strongly influenced by regional temperature and hydrological variations. This variability is potentially driven by high-latitude atmospheric circulation patterns and particularly by the strength of the Siberian High. An increase in its strength indeed can cause colder and potentially drier conditions at the Alilica site. Accordingly, also increased snow cover during early winter would have shortened the season of plant growth, depressing the soil biological activity and influencing the $\delta^{13}\text{C}$ record.



5.2. The growth rate

Three main factors combine to determine speleothem growth rates: the calcium ion concentration, the temperature of the dripwater, and the water supply rate (e.g. Genty et al., 2001b). For time periods of constant vegetation, as assumed for the Alilica catchment during the considered time span, growth-rate variations likely depend on soil CO₂ production, which in turn has the potential to correlate with surface temperature (Genty et al., 2001b) and water availability (Regattieri et al., 2016a). In LID1 the general pattern of the growth rate broadly resembles that of the $\delta^{13}\text{C}$ (Fig. 4), confirming that they are governed, to some extent, by similar processes, i.e. mostly to the degree of soil development in the catchment. The major growth rate decrease at ca. 6.6 ka also resembles an inflection point in both SCAR and GISP2 curves (Fig. 6), indicating colder temperature/drier conditions. However, both the latter curves as well as the LID1 $\delta^{13}\text{C}$ record recover afterwards, whereas growth rate remains consistently lower in the second part of the record (Fig. 4). Interestingly, this major change in accumulation rate is almost coincident with the end of the wettest period identified in speleothem record from the western (Corchia Cave, Zanchetta et al., 2007; Renella Cave, Zhorniyak et al., 2011) and the eastern Mediterranean (Soreq Cave, Bar-Matthews et al., 2000; Bar-Matthews & Ayalon, 2011), partly overlapping with the deposition of Sapropel S1 in the Eastern Mediterranean. This suggests that LID1 growth rate responded sensitively to regional hydrological variations, as well as, potentially, to changes in local temperature.

5.3 The $\delta^{18}\text{O}$ record

The oxygen isotope composition of calcite is by far the most widely used proxy in speleothem studies (e.g. Lachniet, 2009). Assuming a deposition close to the isotopic equilibrium, as suggested by the compact columnar fabric of LID1 (Frisia et al., 2000), and the absence of diagenetic processes, the speleothem $\delta^{18}\text{O}$ depends on the $\delta^{18}\text{O}$ composition of the drip water and on the temperature at which the speleothem precipitated. A well-defined coefficient of $-0.177\text{‰ }^{\circ}\text{C}^{-1}$ was empirically derived for speleothem calcite (Tremaine et al., 2011) and appears only slightly lower with respect that of $-0.206\text{‰ }^{\circ}\text{C}^{-1}$ derived from laboratory experiment by Kim & O'Neil (1997). The $\delta^{18}\text{O}$ of the drip water, in relatively deep caves from temperate to arid settings, appears to mostly represent the weighted mean annual $\delta^{18}\text{O}$ value of precipitation, $\delta^{18}\text{O}_p$, (e.g. Matthey et al., 2008; Baneschi et al., 2011). In the absence of cave monitoring data, and notwithstanding the limitation of this assumption, we can assume that the same holds for Alilica Cave. Factors driving the $\delta^{18}\text{O}_p$, and thus that of the speleothem calcite ($\delta^{18}\text{O}$) are multiple and vary on a

spatial and temporal basis (e.g. Dansgaard, 1964; Lachniet, 2009; Drăguşin et al., 2014; Perşoiu et al., 2017). In most of the Mediterranean region, lower $\delta^{18}\text{O}$ values during wetter periods are commonly reported from speleothems and also from lacustrine carbonates (e.g. Bar-Matthews et al., 2000; Columbu et al., 2017; Drysdale et al., 2005, 2006, 2007; Finné et al., 2014; Regattieri et al., 2015; 2016b, 2017; Roberts et al., 2008; Zanchetta et al., 2012). This is due to the so-called amount effect, an empirical inverse relationship observed between the amount of precipitation and their $\delta^{18}\text{O}_p$ (ca. -2.0‰ per 100 mm/month, Bard et al., 2002), and to the negligible effects of temperature during precipitation condensation (which has a gradient of $+0.3\text{‰}^{\circ}\text{C}^{-1}$), i.e. similar but opposite to the temperature effect during carbonate deposition (Bard et al., 2002). Conversely, $\delta^{18}\text{O}_p$ in central and northern Europe is strongly correlated to temperature ($+0.58\text{‰}^{\circ}\text{C}$, Rozanski et al., 1993), and this leads to a positive relationship between temperature and speleothem $\delta^{18}\text{O}$ (Boch et al., 2011; Koltai et al., 2017; Constantin et al., 2007; Spötl et al. 2006). Thus, the two main drivers of speleothem $\delta^{18}\text{O}$ can be hydrology or temperature, depending mostly on the cave location. However, other effects may influence the final $\delta^{18}\text{O}$ values. For example, changes in the seasonal distribution of the precipitation may lead to a bias toward more positive (if summer precipitation dominates) or more negative (if most of the recharge occurs during winter) mean annual value of cave water $\delta^{18}\text{O}$ and thus of the forming calcite. Also, changes in the location and/or in the isotopic composition of the source of precipitation may strongly impact the final $\delta^{18}\text{O}$ values (Bar-Matthews et al., 2000). The influences of these effects are often difficult to disentangle and may be contrasting or may change during time. This, in some cases, makes it impossible to correctly identify a main driver for the observed $\delta^{18}\text{O}$ variability and thus to assign a proper paleoclimatic interpretation to speleothem oxygen records (e.g. Drăguşin et al., 2014). In the case of LID1 $\delta^{18}\text{O}$, the broad similarity observed with the carbon record and the occurrence of the most positive values during the major growth rate reduction (Fig. 4), together with the absence of correlation with the general pattern of the SCAR temperature record (Fig. 6) suggest that a dominant influence of temperature variations is unlikely. This is also supported by other speleothem oxygen records from southern Balkans (e.g. Finné et al., 2014; Psomiadis et al., 2018) and specifically from Macedonia (Regattieri et al., 2018), all showing a negligible influence of temperature and a general dependence from hydrology.

To disentangle the potential hydrological implications, it is useful to compare the LID1 $\delta^{18}\text{O}$ record with other paleo-hydrological records for which a main driver of variability has been already proposed. Fig. 6 shows

<<<<<< -----

Fig. 6 - Comparison of the LID1 $\delta^{13}\text{C}$ record (A, this study) with $\delta^{18}\text{O}$ record of ice from Scariscoara Cave (B, Perşoiu et al., 2017); with K content from Greenland GISP2 ice core (C, Mayewski et al., 1997), SH is Siberian high; with LID1 $\delta^{18}\text{O}$ (D, this study); $\delta^{18}\text{O}$ record from Soreq Cave (E, Israel, Bar-Matthews et al., 2011); $\delta^{18}\text{O}$ record from Cueva de Asul (F, Northern Spain, Smith et al., 2016). Grey dashed lines indicate common dry/cold intervals identified among the different records.

the comparison with the $\delta^{18}\text{O}$ record from Soreq Cave (Israel, Bar-Matthews & Ayalon, 2011, Fig. 1). At Soreq, the amount effect is considered to control speleothem $\delta^{18}\text{O}$, with winter precipitation largely dominating the annual mean (Bar-Matthews et al., 2000; Bar-Matthews & Ayalon, 2011). The main source of precipitation for western Israel is local cyclogenesis in the Aegean Sea, which is linked to the same synoptic system generating cyclogenesis in the Gulf of Genoa, in turn related to North Atlantic storm tracks (Trigo et al., 2002). Changes in the isotopic composition of the eastern Mediterranean surface water play an important role too in the $\delta^{18}\text{O}$ of Soreq speleothem. These changes are particularly prominent during periods of sapropel deposition (Bar-Matthews et al., 2000), as between 10 ka and 6 ka when the Sapropel S1 was deposited. During these intervals, enhanced fresh-water discharge from the Nile River was induced by strengthening of the African monsoon rainfall over the Nile catchment. It caused ^{18}O -depleted values in the eastern Mediterranean surface water, leading to ^{18}O -depleted composition of Soreq speleothem (Bar-Matthews et al., 2000). The comparison of LID1 and Soreq records (Fig. 6) shows some interesting features: for the first part of the record, when the growth rate of LID1 was higher and the Sapropel S1 was deposited in the eastern Mediterranean, the two records do not show any convincing covariation, likely because changes in the surface water $\delta^{18}\text{O}$ did not affect precipitation at LID site but are prevalent in the case of Soreq Cave during the sapropel deposition. Instead, after ca. 6.6 ka, a broad similarity appears to be present within combined uncertainties (Fig. 6), particularly regarding the interval of positive values centred at ca. 6.5 ka and the general pattern of more positive $\delta^{18}\text{O}$ composition between ca. 6 and 4.5 ka (Fig. 6). This adds support to the hydrological interpretation of the LID1 oxygen record. Another interesting comparison is with the $\delta^{18}\text{O}$ record from Asil Cave (Northern Spain, Smith et al., 2016, Fig. 6). At this site, the speleothem $\delta^{18}\text{O}$ variability has been interpreted in terms of the amount of precipitation over northern Iberia, in turn related to the position and strength of westerly winds bringing moisture from the mid-latitudes of the North Atlantic (Smith et al., 2016). Stronger westerlies/higher precipitation/lower $\delta^{18}\text{O}_p$ over Iberia are observed when the atmospheric pressure gradients are weaker, and the zonal flow is shifted southward. This atmospheric pattern resembles conditions occurring on shorter time scale during negative NAO phases, (NAO⁻-like, Smith et al., 2016; Sánchez-Goñi et al., 2016). Conversely, NAO⁺-like periods are characterized by lower precipitation, and thus by higher speleothem $\delta^{18}\text{O}$ values (Smith et al., 2016). The comparison between LID1 $\delta^{18}\text{O}$ and the Asil records does not show major similarities in their general trends (Fig. 6). However, two almost coeval intervals of more positive $\delta^{18}\text{O}$ values centred at ca. 6.5 ka and 4.6 ka are apparent, within uncertainties, in both records (Fig. 6). This suggests that westerly circulation and NAO-like patterns of atmospheric variability and associated rainfall variations are not the main driver for $\delta^{18}\text{O}$ variability observed at the Alilica site, though an influence can be inferred during specific periods.

Overall the LID1 $\delta^{18}\text{O}$ signal is likely related to hydrological variations, and potentially mostly to the amount effect. However, it is not possible to establish a straightforward link with supra-regional climate patterns, though similarities with the record of westerlies strength and position are apparent during some intervals (e.g. around 6.5 and 4.6 ka). This is due to the complexity of the climate in the Balkan Peninsula, which is under the influence of both Mediterranean and Central Europe atmospheric dynamics, which may cause changes in source and seasonality of the precipitation. Also, these main atmospheric patterns may have a contrasting influence and their boundaries may change over time. For example, as noted above, the strengthening of the Siberian High causes dry winter conditions in the Balkans, but also stimulates the Mediterranean cyclogenesis which brings moisture toward this region. Thus, depending on where the boundary between these two contrasting influences is located, the effect on the local hydrology can be opposite. It is also worth noting that at the Alilica site (i.e. well within the land interior and located in a rainshadow area within the mountains) the influence of the local topography and the development of local thermal low-pressure centres could trigger cyclogenesis to occur locally, strongly imprinting the mean annual $\delta^{18}\text{O}$ values of the precipitation (Trigo et al., 2002). Despite the fact that the interpretation of the oxygen record is complicated by these factors, the similarities observed in specific intervals with the carbon record, as well as with the records used for comparison, may deserve some more attention, and will be addressed in Section 6.

5.4. Frequency of variability

Persistent frequencies highlighted by spectral analyses may give some clues on forcing mechanisms behind climate change processes. Spectral analyses of Holocene records have often identified solar variability as the factor most likely responsible for decadal up to millennial periodicities observed in many records (e.g. Bond et al., 2001; Fletcher et al., 2013; Debret et al., 2009; Meeker & Mayewsky, 2002). During the early Holocene, a 1000-900 yr periodicity has been observed in numerous North Atlantic, Northern Hemisphere and Mediterranean palaeoclimate records, as well as in solar irradiance proxies ($\Delta^{14}\text{C}$ and ^{10}Be) (Fletcher et al., 2013; Debret et al., 2009; Domínguez-Villar et al., 2008). Periodicities of ca. 400-500 yr also have been documented in residual atmospheric ^{14}C production data (e.g. Stuiver & Braziunas, 1993) and were related to solar modulation. On higher frequencies, solar cycles of ~210 yr, ~88 yr, and ~11 yr appear to be strong in Holocene records (Steinilber et al., 2012).

Regarding other potential forcing of variability and their cyclicities, a 1500-year climate cycle appears pervasive in the high latitudes of the North Atlantic (Bianchi & McCave, 1999; Bond et al., 2001), and it is likely linked with internal oscillations of the oceanic circulation (Debret et al., 2007).

For LID1, the three main trends (A= ~1000 yr; B= ~200 yr, C= ~75-100) identified in the carbon and oxygen CWT spectra (Fig. 5) closely approximate main

periodicities addressed to solar forcing, although the shorter periodicity may not be fully significant in our record due to the large associated temporal uncertainties and to the temporal resolution of the record. To disentangle the causal relationship which relates the solar forcing to the $\delta^{18}\text{O}$ variability can be difficult. However, the observed similarities suggest at least an indirect relationship, likely related to solar modulation of large-scale climate patterns and their effects on local climate parameters like temperature, precipitation amount and seasonality (Scholz et al., 2012). For example, a highly persistent power close to ~80-110 years in the K record from Greenland appears to dominate the strength of Siberian High, and was related to solar variability (Meeker & Mayewski, 2002). Interestingly, non-linear relationships between solar intensity and the magnitude of responses of atmospheric circulation features have been proposed, with higher atmospheric responses when overall solar intensity is lowest (Meeker & Mayewski, 2002). This may account for changes in intensity observed in trends B and C. Instead, the shift between trends A1 and A2 (i.e. from 1000 to 1200-1500 yr), resembles what was observed around 6 ka in many Holocene records (Fletcher et al., 2013; Debret et al., 2009; Domínguez-Villar et al., 2008), although in the LID1 record it could not be considered fully representative due to the total length of the record and to the influence of edge effects. Interestingly, the lower-frequency cyclicity after ca. 6 ka has been related in the Mediterranean to shifts between a prevailing strong and weak state of the zonal flow, with impacts similar to the positive and negative modes of the present-day North Atlantic Oscillation (NAO-like patterns, Fletcher et al., 2013).

6. REGIONAL SIGNIFICANCE OF THE LID1 RECORD

The comparison of the LID1 record with regional and extra-regional temperature and hydrological records shows both similarities and differences (Fig. 6), which can be addressed by considering the interplay of local conditions with large-scale climatic patterns. Regarding the general patterns, the $\delta^{13}\text{C}$ record shows a decreasing trend, which following our interpretation indicates warmer and wetter conditions between the beginning of the record and up to ca. 7.6 ka. This trend resembles the warming trend observed in the temperature record from SCAR and a decrease in the intensity of the Siberian High (Fig. 6). We may speculate that this trend towards an amelioration of climate conditions is related to the recovery after the so-called 8.2 event (e.g. Alley et al. 1997), a widespread cold and dry interval recognized in many records from the Northern Hemisphere and specifically in the Mediterranean (e.g. Pross et al., 2009). Instead, the oxygen record does not show any well-defined trend, either in the first and in the second portion of the record. For example, the widespread drying trend reported from speleothems and lakes in the Mediterranean since ca. 5-6 ka (e.g. Roberts et al., 2008) is not apparent in the LID1 record. Up to ca. 6.6 ka the $\delta^{18}\text{O}$ pattern appears also largely decoupled from the $\delta^{13}\text{C}$ record, as well as from the regional hydro-climatic framework (Fig. 6). This is potentially due to the

overriding influence of local orographic/thermal effects and/or to changes in the season of cave recharge. However, a stronger degree of coherency with the $\delta^{13}\text{C}$ record and with the regional situation is observed in the younger portion of the $\delta^{18}\text{O}$ record, from ca. 6.7 ka onward, and especially for specific intervals (Fig. 6). Interestingly, the change in the $\delta^{18}\text{O}$ pattern between ca. 6.5 and 6.7 ka corresponds to a dramatic and permanent decrease in the growth rate, coincident to the end of the wettest period identified in the speleothem oxygen record at Corchia Cave (Central Italy; Zanchetta et al., 2007) and related to regional winter precipitation increases during the deposition of sapropel S1. At 6.5 ka all the LID1 proxies indicate a colder and drier interval. This event is also apparent in the hydrological record from Soreq Cave and potentially relates to an interval of persistent NAO⁺-like conditions, as indicated by the speleothem record from Cueva de Asiuil (Northern Iberia, Smith et al., 2016, Fig. 6). Interestingly, this event is also present in the Romanian temperature record (Fig. 6), but it is not prominent at all in the record of Siberian High strength (Fig. 6), suggesting a prevailing atmospheric forcing originating in the North Atlantic Region which propagated southward and eastward. Interestingly, the drier event at 6.5 ka in the Soreq record was also related to an important cultural transition recorded from archaeological records in the eastern Mediterranean (i.e. from Mid to Late Chalcolithic period, Bar-Matthews & Ayalon, 2011), adding support to its significance in the region. It also corresponds, within combined uncertainties, to a period of rapid climate change (RCC's), as identified by Mayewski et al (2004) from a compilation of 50 globally distributed records. Most of the climate change occurring during RCC's appears characterized by polar cooling, tropical aridity, and major atmospheric circulation changes (Mayewski et al., 2004), and thus generally drier conditions within the Mediterranean fits well with this general background. Also the compilation from Wanner et al. (2011) highlights the occurrence of a cold event of global significance centered at ca. 6.3 ka. During this event a remarkable dryness existed in the Asian monsoon area between about 6.9 and 6.3 ka and it was argued that East Asian monsoon was extremely weak due to a cold North Atlantic area and a southward shift of the ITCZ (Wanner et al., 2011). After a brief recovery of precipitation and temperature, another event is coherently expressed by the two stable isotope series of LID1 at ca. 5.8 ka. It appears marked by strong temperature reduction in the SCAR record, and is associated with a strong increase in the activity of the Siberian High (Fig. 6), as well as by a reduction of precipitation in the Soreq area (Fig. 6). Interestingly, it does not appear associated with changes in atmospheric conditions related to NAO-like patterns (Fig. 6). This may suggest a prevailing influence of eastern and high-latitudes atmospheric patterns, with the expansion of the Siberian High directly influencing precipitation and temperature in the southern Balkans. Another interval of reduced temperature and possibly precipitation is apparent at ca. 5.4 ka. It matches, within uncertainties, the 5.6 ka dry event identified in the Soreq record but also in the $\delta^{18}\text{O}$ record from Corchia Cave (Central Italy, Zanchetta et al.,

2014). This event was correlated to a coeval phase of elevated wind strength inferred from the grain-size record from the Hólmsá loess profile in Iceland (Jackson et al. 2005), corresponding to enhanced westerly flows under persistent NAO⁺-like condition (Zanchetta et al., 2014). Coherently with this interpretation, it also corresponds to a decrease in precipitation expressed by the Cueva de Asiul record (Fig. 6, Smith et al., 2016), but not to either a particular decrease in central Europe temperature or to a strong increase in the activity of the Siberian High (Fig. 6), suggesting again a North-Atlantic source of hydro-climate variability. The last event, occurring at 4.5 ka, is expressed as colder and drier in the LID1 record and it is associated with a major increase in the Siberian High strength and to a strong temperature reduction in the Romanian temperature record (Fig. 6). It is also marked by persistent NAO⁺-like conditions (Fig. 6). This suggests that during this interval the LID1 site was predominantly under the influence North-Atlantic-Mediterranean circulation, potentially indirectly influenced by the strength of the Siberian High. However, it must be noted that this event is not clearly expressed by the Soreq record. Evidence for a cold period around 4.7 ka was proposed as well from the compilation by Waner et al. (2011). The LID1 records ends at 4.1 ka and immediately before drier and colder conditions appear clearly expressed by the two isotope series. We suggest that this latter period of climatic deterioration at the LID1 site corresponds to the widespread 4.2 event, which has been widely recognized in paleoclimatic record from the Northern Hemisphere (e.g. Cullen et al., 2000; Drysdale et al., 2006; Zanchetta et al., 2016). It may also be coherent with the end of LID1 deposition, potentially due to colder/drier conditions which inhibits speleothem growth, though speleothems can cease to grow also for causes which are not climate-related (e.g. for obsolescence or closure of the drip-feeding path related to the evolution of the recharge system).

7. CONCLUDING REMARKS

In this work we have presented a stable isotope and growth rate record from a stalagmite, LID1, which grew between 8.3 ka and 4.1 ka in the Alilica Cave, in the F.Y.R.O.M (southern Balkans). The $\delta^{13}\text{C}$ record appears to be related to the degree of soil development in the cave catchment. The comparison with a highly resolved temperature record reconstructed from $\delta^{18}\text{O}$ of ice from Scărișoara Cave, in western Romania, (Perșoiu et al., 2017) and with the K content of the Greenland GISP ice core (Mayevski et al., 1997), a proxy for the strength of the Siberian High (a semi-permanent anticyclonic area which influences winter and autumn temperature in a large part of the Northern Hemisphere as well as precipitation in Eastern and central Europe, e.g. Panagiotopoulos et al., 2005), suggests that the $\delta^{13}\text{C}$ of LID1 is influenced by regional temperature and hydrological variations, especially since ca. 6.7 ka (Fig. 6). Intervals of increased $\delta^{13}\text{C}$ corresponding to temperature reductions in the Scărișoara record are apparent at ca. 7.1 ka, 6.5 ka, 5.8 ka, 5.4 ka and 4.5 ka (Fig. 6). Most of these events also correspond to intervals of

increased strength of the Siberian High. The proposed mechanism is that such strengthening causes an increase in the occurrence of north-easterly outbursts of cold polar air (Rohling et al., 2002), exerting a downstream effect on regional winter temperature and precipitation in the Balkan Peninsula and depressing the soil biological activity at the LID1 site. This relationship seems to be confirmed by the growth-rate record, which shows a general pattern similar to the $\delta^{13}\text{C}$ record, both being related to CO_2 supply from soil. Interestingly, the long-term trend of the growth rate, which shows a major and permanent reduction at ca. 6.7 ka, appears to be strongly influenced by regional hydrology, with the major decrease corresponding to the end of the wettest period highlighted by speleothem records from western and eastern Mediterranean (Zanchetta et al., 2007; Bar-Matthews et al., 2000). The $\delta^{18}\text{O}$ record broadly resembles that of the carbon, especially for the centennial scale variability and particularly since 6.7 ka (Figs. 4 and 6). This, and the absence of positive correlation with the Scărișoara record, allows us to rule out a temperature dependency for the $\delta^{18}\text{O}$ variability, which appears related to overall hydrological variations, and potentially mostly to the amount effect. However, it is not possible to establish an unequivocal link with supra-regional climate patterns, possibly due to the overriding influence of local orographic/thermal effects on the $\delta^{18}\text{O}$ of precipitation. These effects appear to dominate especially in the first part of the record (i.e. before ca. 6.7 ka), where the $\delta^{18}\text{O}$ record appears largely decoupled from the regional conditions. In this portion it is likely that the $\delta^{18}\text{O}$ signal is buffered by multiple and contrasting processes, which make the climatic signal difficult to disentangle. Later, although a unequivocal forcing for the observed variability is still difficult to constrain, more similarities with the regional situation are observed (Fig. 6), and especially more positive $\delta^{18}\text{O}$ spikes at ca. 6.5 ka, 5.8 ka and 4.5 ka can be linked to regionally-recognized events of reduced precipitation. A combined influence of North Atlantic-Mediterranean atmospheric patterns versus eastern high-latitude dynamics driven by the Siberian High may be suggested, and changes in the boundary between these two influences likely are responsible for the complex pattern observed. Overall, the presented LID1 record adds a piece in the puzzle of the regional paleoclimatic framework for the Middle Holocene in the Mediterranean region. Finally, the occurrence of periodicities similar to those related to solar activity also suggests a solar modulation of large-scale climate patterns, exerting effects on local climate parameters like temperature, precipitation amount and seasonality.

ACKNOWLEDGMENTS

This paper is the result of CCALMA (Climate from CAves and Lakes in Macedonia) working group, which paralleled the development of the SCOPSCO-ICDP project on Lake Ohrid. This work has been partly funded by the Australian Research Council Discovery Project DP160102969ARC. We thank the Mavrovo National Park and the Speleological Society "Peoni" from Skopje for the warm logistic support during field work. We also thank A. Perșoiu for providing SCAR data. We greatly

thank A.E. Fallick and another anonymous reviewer for their positive comments.

REFERENCES

- Alley R.B., Mayewski P.A., Sowers T., Stuiver M., Taylor K.C., Clark P.U. (1997) - Holocene climatic instability: A prominent, widespread event 8200 yr ago. *Geology*, 25(6), 483-486.
- Andonovski T. (1980) - Cave system Alilica. Sedmi Jugoslovenski speleološki kongres. Speleološko društvo SR Crne Gore, 21-30 (in Macedonian).
- Andonovski T., Manakovik D., Stojmilov A., Stojanovik M., (1998) - Geomorfološka karta na Republika Makedonija. Prosvetno Delo, Skopje (in Macedonian).
- Bajo P., Borsato A., Drysdale R., Hua Q., Frisia S., Zanchetta G., Woodhead J. (2017) - Stalagmite carbon isotopes and dead carbon proportion (DCP) in a near-closed-system situation: An interplay between sulphuric and carbonic acid dissolution. *Geochimica et Cosmochimica Acta*, 210, 208-227.
- Baneschi I., Piccini L., Regattieri E., Isola I., Guidi M., Lotti L., Zanchetta G. (2011) - Hypogean microclimatology and hydrology of the 800-900 m asl level in the Monte Corchia cave (Tuscany, Italy): preliminary considerations and implications for paleoclimatological studies. *Acta Carsologica*, 40(1), 175-187.
- Bard E., Delaygue G., Rostek F., Antonioli F., Silenzi S., Schrag D.P. (2002) - Hydrological conditions over the western Mediterranean basin during the deposition of the cold Sapropel 6 (ca. 175 kyr BP). *Earth and Planetary Science Letters*, 202(2), 481-494.
- Bar-Matthews M., Ayalon A., Kaufman A. (2000) - Timing and hydrological conditions of Sapropel events in the Eastern Mediterranean, as evident from speleothems, Soreq cave, Israel. *Chemical Geology*, 169(1-2), 145-156.
- Bar-Matthews M., Ayalon A. (2011) - Mid-Holocene climate variations revealed by high-resolution speleothem records from Soreq Cave, Israel and their correlation with cultural changes. *The Holocene*, 21(1), 163-171.
- Bianchi G.G., McCave I.N. (1999) - Holocene periodicity in North Atlantic climate and deep-ocean flow south of Iceland. *Nature*, 397(6719), 515.
- Boch R., Cheng H., Spötl C., Edwards R.L., Wang X., Häuselmann P. (2011) - NALPS: a precisely dated European climate record 120-60 ka. *Climate of the past*, 7(4), 1247-1259.
- Bond G., Showers W., Cheseby M., Lotti R., Almasi P., Priore P., Bonani G. (1997) - A pervasive millennial-scale cycle in North Atlantic Holocene and glacial climates. *Science*, 278(5341), 1257-1266.
- Bond G., Kromer B., Beer J., Muscheler R., Evans M. N., Showers W., Bonani G. (2001) - Persistent solar influence on North Atlantic climate during the Holocene. *Science*, 294(5549), 2130-2136.
- Cohen J., Entekhabi D. (1999) - Eurasian snow cover variability and Northern Hemisphere climate predictability. *Geophysical Research Letters*, 26(3), 345-348.
- Columbu A., Drysdale R., Capron E., Woodhead J., De Waele J., Sanna L., Bajo P. (2017) - Early last glacial intra-interstadial climate variability recorded in a Sardinian speleothem. *Quaternary Science Reviews*, 169, 391-397.
- Constantin S., Bojar A.V., Lauritzen S.E., Lundberg J. (2007) - Holocene and Late Pleistocene climate in the sub-Mediterranean continental environment: a speleothem record from Poleva Cave (Southern Carpathians, Romania). *Palaeogeography, Palaeoclimatology, Palaeoecology*, 243(3-4), 322-338.
- Cremaschi M., Mercuri A.M., Torri P., Florenzano A., Pizzi C., Marchesini M., Zerboni A. (2016) - Climate change versus land management in the Po Plain (Northern Italy) during the Bronze Age: New insights from the VP/VG sequence of the Terramara Santa Rosa di Poviglio. *Quaternary Science Reviews*, 136, 153-172.
- Cullen H.M., deMenocal P.B., Hemming S., Hemming G., Brown F.H., Guilderson T., Sirocko F. (2000) - Climate change and the collapse of the Akkadian empire: Evidence from the deep sea. *Geology*, 28(4), 379-382.
- Dansgaard W. (1964) - Stable isotopes in precipitation. *Tellus*, 16(4), 436-468.
- Debret M., Bout-Roumazielles V., Grousset F., Desmet M., McManus J.F., Massei N., Trentesaux A. (2007) - The origin of the 1500-year climate cycles in Holocene North-Atlantic records. *Climate of the Past*, 3, 569-575.
- Debret M., Sebag D., Crosta X., Massei N., Petit J.R., Chapron E., Bout-Roumazielles V. (2009) - Evidence from wavelet analysis for a mid-Holocene transition in global climate forcing. *Quaternary Science Reviews*, 28(25-26), 2675-2688.
- Domínguez-Villar D., Wang X., Cheng H., Martín-Chivelet J., Edwards R.L. (2008) - A high-resolution late Holocene speleothem record from Kaite Cave, northern Spain: $\delta^{18}\text{O}$ variability and possible causes. *Quaternary International*, 187(1), 40-51.
- Drăguşin V., Staubwasser M., Hoffmann D.L., Ersek V., Onac B.P., Vereş D. (2014) - Constraining Holocene hydrological changes in the Carpathian-Balkan region using speleothem $\delta^{18}\text{O}$ and pollen-based temperature reconstructions. *Climate of the Past*, 10, 1363.
- Drysdale R.N., Zanchetta G., Hellstrom J.C., Fallick A. E., Zhao J.X. (2005) - Stalagmite evidence for the onset of the Last Interglacial in southern Europe at 129 ± 1 ka. *Geophysical Research Letters*, 32(24).
- Drysdale R., Zanchetta G., Hellstrom J., Maas R., Fallick A., Pickett M., Piccini L. (2006) - Late Holocene drought responsible for the collapse of Old-World civilizations is recorded in an Italian cave flowstone. *Geology*, 34(2), 101-104.
- Drysdale R.N., Zanchetta G., Hellstrom J.C., Fallick A.E., McDonald J., Cartwright I. (2007) - Stalagmite evidence for the precise timing of North Atlan-

- tic cold events during the early last glacial. *Geology*, 35(1), 77-80.
- Dünkeloh A., Jacobeit J. (2003) - Circulation dynamics of Mediterranean precipitation variability 1948-98. *International Journal of Climatology*, 23(15), 1843-1866.
- Fairchild I.J., Smith C.L., Baker A., Fuller L., Spötl C., Matthey D., McDermott F. (2006) - Modification and preservation of environmental signals in speleothems. *Earth-Science Reviews*, 75(1-4), 105-153.
- Finné M., Bar-Matthews M., Holmgren K., Sundqvist H.S., Liakopoulos I., Zhang Q. (2014) - Speleothem evidence for late Holocene climate variability and floods in Southern Greece. *Quaternary Research*, 81(2), 213-227.
- Fletcher W.J., Debret M., Sánchez-Goñi M.F. (2013) - Mid-Holocene emergence of a low-frequency millennial oscillation in western Mediterranean climate: Implications for past dynamics of the North Atlantic atmospheric westerlies. *The Holocene*, 23(2), 153-166.
- Frisia S., Borsato A., Fairchild I.J., McDermott F. (2000) - Calcite fabrics, growth mechanisms, and environments of formation in speleothems from the Italian Alps and southwestern Ireland. *Journal of Sedimentary Research*, 70(5), 1183-1196.
- Genty D., Baker A., Massault M., Proctor C., Gilmour M., Pons-Branchu E., Hamelin B. (2001a) - Dead carbon in stalagmites: carbonate bedrock paleodissolution vs. ageing of soil organic matter. Implications for ^{13}C variations in speleothems. *Geochimica et Cosmochimica Acta*, 65(20), 3443-3457.
- Genty D., Baker A., Vokal B. (2001b) - Intra- and inter-annual growth rate of modern stalagmites. *Chemical Geology*, 176(1-4), 191-212.
- Giorgi F., Lionello P. (2008) - Climate change projections for the Mediterranean region. *Global and Planetary Change*, 63(2-3), 90-104.
- Giraudi C., Magny M., Zanchetta G., Drysdale R.N. (2011) - The Holocene climatic evolution of Mediterranean Italy: A review of the continental geological data. *The Holocene*, 21(1), 105-115.
- Hellstrom J. (2003) - Rapid and accurate U/Th dating using parallel ion-counting multi-collector ICP-MS. *Journal of Analytical Atomic Spectrometry*, 18(11), 1346-1351.
- Hellstrom J. (2006) - U-Th dating of speleothems with high initial ^{230}Th using stratigraphical constraint. *Quaternary Geochronology*, 1(4), 289-295.
- Jackson M.G., Oskarsson N., Trønnnes R.G., McManus J.F., Oppo D.W., Gronvold K., Sachs J.P. (2005) - Holocene loess deposition in Iceland: Evidence for millennial-scale atmosphere-ocean coupling in the North Atlantic. *Geology*, 33(6), 509-512.
- Jalut G., Dedoubat J.J., Fontugne M., Otto T. (2009) - Holocene circum-Mediterranean vegetation changes: climate forcing and human impact. *Quaternary International*, 200(1-2), 4-18.
- Karamata S. (2006) - The geological development of the Balkan Peninsula related to the approach, collision and compression of Gondwanan and Eurasian units. *Geological Society, London, Special Publications*, 260(1), 155-178.
- Kim S.T., O'Neil J.R. (1997) - Equilibrium and nonequilibrium oxygen isotope effects in synthetic carbonates. *Geochimica et Cosmochimica Acta*, 61, 3461-3475.
- Koltai G., Spötl C., Shen C.C., Wu C.C., Rao Z., Palcsu L., Bárányi-Kevei I. (2017) - A penultimate glacial climate record from southern Hungary. *Journal of Quaternary Science*, 32(7), 946-956.
- Lachniet M.S. (2009) - Climatic and environmental controls on speleothem oxygen-isotope values. *Quaternary Science Reviews*, 28(5-6), 412-432.
- López-Moreno J.I., Vicente-Serrano S.M., Morán-Tejeda E., Lorenzo-Lacruz J., Kenawy A., Beniston M. (2011) - Effects of the North Atlantic Oscillation (NAO) on combined temperature and precipitation winter modes in the Mediterranean mountains: observed relationships and projections for the 21st century. *Global and Planetary Change*, 77(1-2), 62-76.
- Magny M., Miramont C., Sivan O. (2002) - Assessment of the impact of climate and anthropogenic factors on Holocene Mediterranean vegetation in Europe on the basis of palaeohydrological records. *Palaeogeography, Palaeoclimatology, Palaeoecology*, 186(1-2), 47-59.
- Matthey D., Lowry D., Duffet J., Fisher R., Hodge E., Frisia S. (2008) - A 53 year seasonally resolved oxygen and carbon isotope record from a modern Gibraltar speleothem: reconstructed drip water and relationship to local precipitation. *Earth and Planetary Science Letters*, 269(1-2), 80-95.
- Mayewski P.A., Meeker L.D., Twickler M.S., Whitlow S., Yang Q., Lyons W. B., Prentice M. (1997) - Major features and forcing of high-latitude northern hemisphere atmospheric circulation using a 110,000-year-long glaciochemical series. *Journal of Geophysical Research: Oceans*, 102(C12), 26345-26366.
- Mayewski P.A., Rohling E.E., Stager J.C., Karlén W., Maasch K.A., Meeker L.D., Lee-Thorp J. (2004) - Holocene climate variability. *Quaternary Research*, 62(3), 243-255.
- Meeker L.D., Mayewski P.A. (2002) - A 1400-year high-resolution record of atmospheric circulation over the North Atlantic and Asia. *The Holocene*, 12(3), 257-266.
- Mickler P.J., Stern L.A., Banner J.L. (2006) - Large kinetic isotope effects in modern speleothems. *Geological Society of America Bulletin*, 118(1-2), 65-81.
- Panagiotopoulos F., Shahgedanova M., Hannachi A., Stephenson D.B. (2005) - Observed trends and teleconnections of the Siberian high: A recently declining center of action. *Journal of Climate*, 18(9), 1411-1422.
- Panagiotopoulos K., Aufgebauer A., Schäbitz F., Wagner B. (2013) - Vegetation and climate history of the Lake Prespa region since the Lateglacial. *Quaternary International*, 293, 157-169.
- Perşoiu A., Onac B.P., Wynn J.G., Blaauw M., Ionita M.,

- Hansson M. (2017) - Holocene winter climate variability in Central and Eastern Europe. *Scientific Reports*, 7(1), 1196.
- Petkovski P., Ivanovski T. (1980) - Geological map and Guide book for sheet Kičevo (K 34-90), Basic Geological Map of SFRJ 1:100000. Federal Geological Survey (in Macedonian with English abstract). Belgrade, pp. 69.
- Piva A., Asioli A., Trincardi F., Schneider R.R., Vigliotti L. (2008) - Late-Holocene climate variability in the Adriatic sea (Central Mediterranean). *The Holocene*, 18(1), 153-167.
- Pross J., Kotthoff U., Müller U.C., Peyron O., Dormoy I., Schmiedl G., Smith A. M. (2009) - Massive perturbation in terrestrial ecosystems of the Eastern Mediterranean region associated with the 8.2 kyr BP climatic event. *Geology*, 37(10), 887-890.
- Psomiadis D., Dotsika E., Albanakis K., Ghaleb B., Hillaire-Marcel C. (2018) - Speleothem record of climatic changes in the northern Aegean region (Greece) from the Bronze Age to the collapse of the Roman Empire. *Palaeogeography, Palaeoclimatology, Palaeoecology*, 489, 272-283.
- Reale M., Lionello P. (2013) - Synoptic climatology of winter intense precipitation events along the Mediterranean coasts. *Natural Hazards and Earth System Sciences*, 13(7), 1707-1722.
- Regattieri E., Zanchetta G., Drysdale R.N., Isola I., Hellstrom J.C., Roncioni A. (2014) - A continuous stable isotope record from the penultimate glacial maximum to the Last Interglacial (159-121 ka) from Tana Che Urla Cave (Apuan Alps, central Italy). *Quaternary Research*, 82(2), 450-461.
- Regattieri E., Giaccio B., Zanchetta G., Drysdale R.N., Galli P., Nomade S., Wulf S. (2015) - Hydrological variability over the Apennines during the Early Last Glacial precession minimum, as revealed by a stable isotope record from Sulmona basin, Central Italy. *Journal of Quaternary Science*, 30(1), 19-31.
- Regattieri E., Zanchetta G., Drysdale R.N., Isola I., Woodhead J.D., Hellstrom J.C., Dotsika E. (2016a) - Environmental variability between the penultimate deglaciation and the mid Eemian: Insights from Tana che Urla (central Italy) speleothem trace element record. *Quaternary Science Reviews*, 152, 80-92.
- Regattieri E., Giaccio B., Galli P., Nomade S., Peronace E., Messina P., Gemelli M. (2016b) - A multiproxy record of MIS 11-12 deglaciation and glacial MIS 12 instability from the Sulmona basin (central Italy). *Quaternary Science Reviews*, 132, 129-145.
- Regattieri E., Giaccio B., Nomade S., Francke A., Vogel H., Drysdale R.N., Boschi C. (2017) - A Last Interglacial record of environmental changes from the Sulmona Basin (central Italy). *Palaeogeography, Palaeoclimatology, Palaeoecology*, 472, 51-66.
- Regattieri E., Zanchetta G., Isola I., Bajo P., Perchiazzi N., Drysdale R.N., Wagner B. (2018) - A MIS 9/ MIS 8 speleothem record of hydrological variability from Macedonia (FYROM). *Global and Planetary Change*, 162, 39-52.
- Roberts N., Jones M. D., Benkaddour A., Eastwood W.J., Filippi M.L., Frogley M.R., Stevens L. (2008) - Stable isotope records of Late Quaternary climate and hydrology from Mediterranean lakes: the ISOMED synthesis. *Quaternary Science Reviews*, 27(25-26), 2426-2441.
- Rogers J.C. (1997) - North Atlantic storm track variability and its association to the North Atlantic Oscillation and climate variability of northern Europe. *Journal of Climate*, 10(7), 1635-1647.
- Rohling E., Mayewski P., Abu-Zied R., Casford J., Hayes A. (2002) - Holocene atmosphere-ocean interactions: records from Greenland and the Aegean Sea. *Climate Dynamics*, 18(7), 587-593.
- Rozanski K., Araguás-Araguás L., Gonfiantini R. (1993) - Isotopic patterns in modern global precipitation. *Climate change in continental isotopic records*, 78, 1-36.
- Sadori L., Jahns S., Peyron O. (2011) - Mid-Holocene vegetation history of the central Mediterranean. *The Holocene*, 21(1), 117-129.
- Sadori L., Koutsodendrīs A., Masi A., Bertini A., Combourieu-Nebout N., Francke A., Peyron O. (2016) - Pollen-based paleoenvironmental and paleoclimatic change at Lake Ohrid (south-eastern Europe) during the past 500 ka. *Biogeosciences*, 13, 1423-1437.
- Sanchez-Goñi M.F., Rodrigues T., Hodell D.A., Polanco-Martinez J.M., Alonso-García M., Hernández-Almeida I., Ferretti P. (2016) - Tropical-driven climate shifts in southwestern Europe during MIS 19, a low eccentricity interglacial. *Earth and Planetary Science Letters*, 448, 81-93.
- Scholz D., Hoffmann D.L. (2011) - StalAge-An algorithm designed for construction of speleothem age models. *Quaternary Geochronology*, 6(3-4), 369-382.
- Scholz D., Frisia S., Borsato A., Spötl C., Fohlmeister J., Mudelsee M., Mangini A. (2012) - Holocene climate variability in north-eastern Italy: potential influence of the NAO and solar activity recorded by speleothem data. *Climate of the Past*, 8(4), 1367-1383.
- Smith A.C., Wynn P.M., Barker P.A., Leng M.J., Noble S.R., Tych W. (2016) - North Atlantic forcing of moisture delivery to Europe throughout the Holocene. *Scientific Reports*, 6, 24745.
- Spötl C., Mangini A., Richards D.A. (2006) - Chronology and paleoenvironment of Marine Isotope Stage 3 from two high-elevation speleothems, Austrian Alps. *Quaternary Science Reviews*, 25(9-10), 1127-1136.
- Steinhilber F., Abreu J. A., Beer J., Brunner I., Christl M., Fischer H., Miller H. (2012) - 9,400 years of cosmic radiation and solar activity from ice cores and tree rings. *Proceedings of the National Academy of Sciences*, 109(16), 5967-5971.
- Stuiver M., Braziunas T.F. (1993) - Modeling atmospheric ^{14}C influences and ^{14}C ages of marine samples to 10,000 BC. *Radiocarbon*, 35(1), 137-189.
- Tognarelli A., Zanchetta G., Regattieri E., Isola I., Drysdale R.N., Bini M., Hellstrom J.C. (2018) -

- Wavelet analysis of $\delta^{18}\text{O}$ and $\delta^{13}\text{C}$ time-series from an Holocene speleothem record from Corchia Cave (central Italy): insights for the recurrence of dry-wet periods in the Central Mediterranean. *Italian Journal of Geosciences*, 137(1), 128-137.
- Tognarelli A. (2018) - The use of continuous wavelet transform for Ground-Roll attenuation. 80th EAGE Conference. Doi 10.3997/2214-4609.201801417
- Tremaine D.M., Froelich P.N., Wang Y. (2011) - Speleothem calcite formed in situ: Modern calibration of $\delta^{18}\text{O}$ and $\delta^{13}\text{C}$ paleoclimate proxies in a continuously-monitored natural cave system. *Geochimica et Cosmochimica Acta*, 75(17), 4929-4950.
- Trigo I.F., Bigg G.R., Davies T.D. (2002) - Climatology of cyclogenesis mechanisms in the Mediterranean. *Monthly Weather Review*, 130(3), 549-569.
- Ulbrich U., Lionello P., Belušić D., Jacobbeit J., Knippertz P., Kuglitsch F.G., Nissen K.M. (2012) - Climate of the Mediterranean: synoptic patterns, temperature, precipitation, winds, and their extremes. In *The Climate of the Mediterranean Region* (pp. 301-346). Eds Lionello, P. Elsevier Insights
- Walker M.J., Berkelhammer M., Björck S., Cwynar L.C., Fisher D.A., Long A.J., Weiss H. (2012) - Formal subdivision of the Holocene Series/Epoch: a Discussion Paper by a Working Group of INTIMATE (Integration of ice-core, marine and terrestrial records) and the Subcommission on Quaternary Stratigraphy (International Commission on Stratigraphy). *Journal of Quaternary Science*, 27(7), 649-659.
- Wanner H., Beer J., Bütikofer J., Crowley T.J., Cubasch U., Flückiger J., Küttel M. (2008) - Mid-to Late Holocene climate change: an overview. *Quaternary Science Reviews*, 27(19-20), 1791-1828.
- Wanner H., Solomina O., Grosjean M., Ritz S.P., Jetel M. (2011) - Structure and origin of Holocene cold events. *Quaternary Science Reviews*, 30(21-22), 3109-3123.
- Xoplaki E., Gonzalez-Rouco J.F., Luterbacher J., Wanner H. (2003) - Mediterranean summer air temperature variability and its connection to the large-scale atmospheric circulation and SSTs. *Climate Dynamics*, 20(7-8), 723-739.
- Zanchetta G., Drysdale R.N., Hellstrom J.C., Fallick A.E., Isola I., Gagan M.K., Pareschi M. T. (2007) - Enhanced rainfall in the Western Mediterranean during deposition of sapropel S1: stalagmite evidence from Corchia cave (Central Italy). *Quaternary Science Reviews*, 26(3-4), 279-286.
- Zanchetta G., Van Welden A., Baneschi I., Drysdale R., Sadori L., Roberts N., Sulpizio R. (2012) - Multi-proxy record for the last 4500 years from Lake Shkodra (Albania/Montenegro). *Journal of Quaternary Science*, 27(8), 780-789.
- Zanchetta G., Bar-Matthews M., Drysdale R.N., Lionello P., Ayalon A., Hellstrom J.C., Regattieri E. (2014) - Coeval dry events in the central and eastern Mediterranean basin at 5.2 and 5.6 ka recorded in Corchia (Italy) and Soreq caves (Israel) speleothems. *Global and Planetary Change*, 122, 130-139.
- Zanchetta G., Regattieri E., Isola I., Drysdale R.N., Bini M., Baneschi I., Hellstrom J.C. (2016) - The so-called "4.2 event" in the central Mediterranean and its climatic teleconnections. *Alpine and Mediterranean Quaternary*, 29(1), 5-17.
- Zhornyak L.V., Zanchetta G., Drysdale R.N., Hellstrom J.C., Isola I., Regattieri E., Couchoud I. (2011) - Stratigraphic evidence for a "pluvial phase" between ca 8200-7100 ka from Renella cave (Central Italy). *Quaternary Science Reviews*, 30(3-4), 409-417.